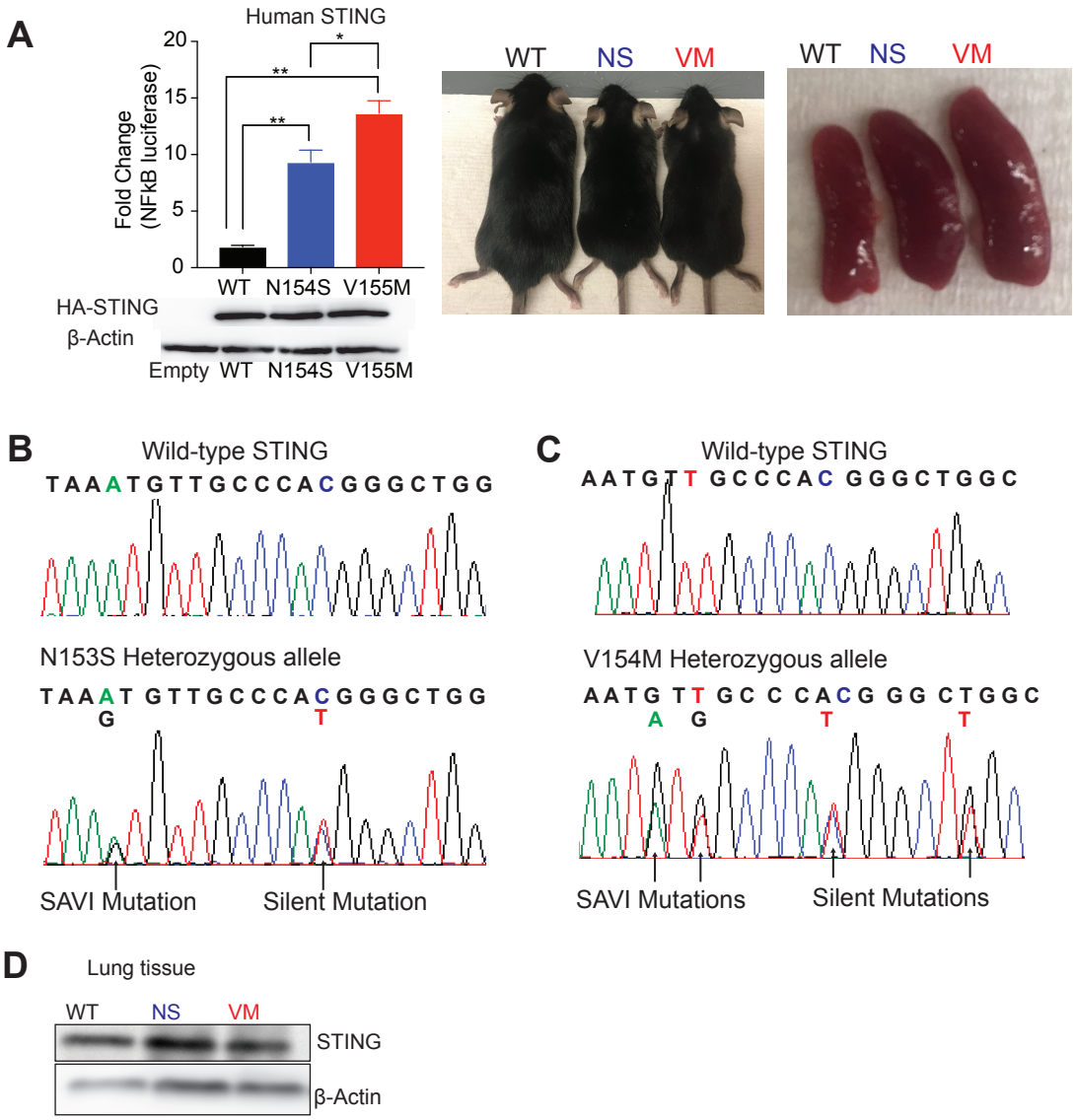

Fig. S1. Reduced survival and spontaneous disease in N153S and V154M SAVI heterozygous mice
293T cells were transfected with plasmid encoding either the human WT or mutant Human STING variants along with NFkB reporter gene (**A, Left)** Representative mouse (**A, Middle**) and spleen pictures (**A, Right**) of 5-week-old males, WT, N153S HET and V154M HET mouse. Visualization of Sanger sequencing to differentiate the WT allele from the N153S HET allele. Nucleotide "A" (**B, upper panel**) in WT allele was mutated to "G" (**B, lower panel**) Nucleotide "C" (**B, upper panel**) to "T" (**B, lower panel**) was a silent mutation. For the V154M HET allele nucleotides "G" and "T" (**C, upper panel**) were mutated to "A" and "G" (**C, lower panel**) Nucleotide "C" (**C, upper panel**) to "T" (**C, lower panel**) and "G" (**C, upper panel**) to "T" (**C, lower panel**) were silent mutations. **(D)** Lysates were prepared from total lung tissue from WT, N153S HET and V154M HET and probed for STING protein and Actin was used as loading control.

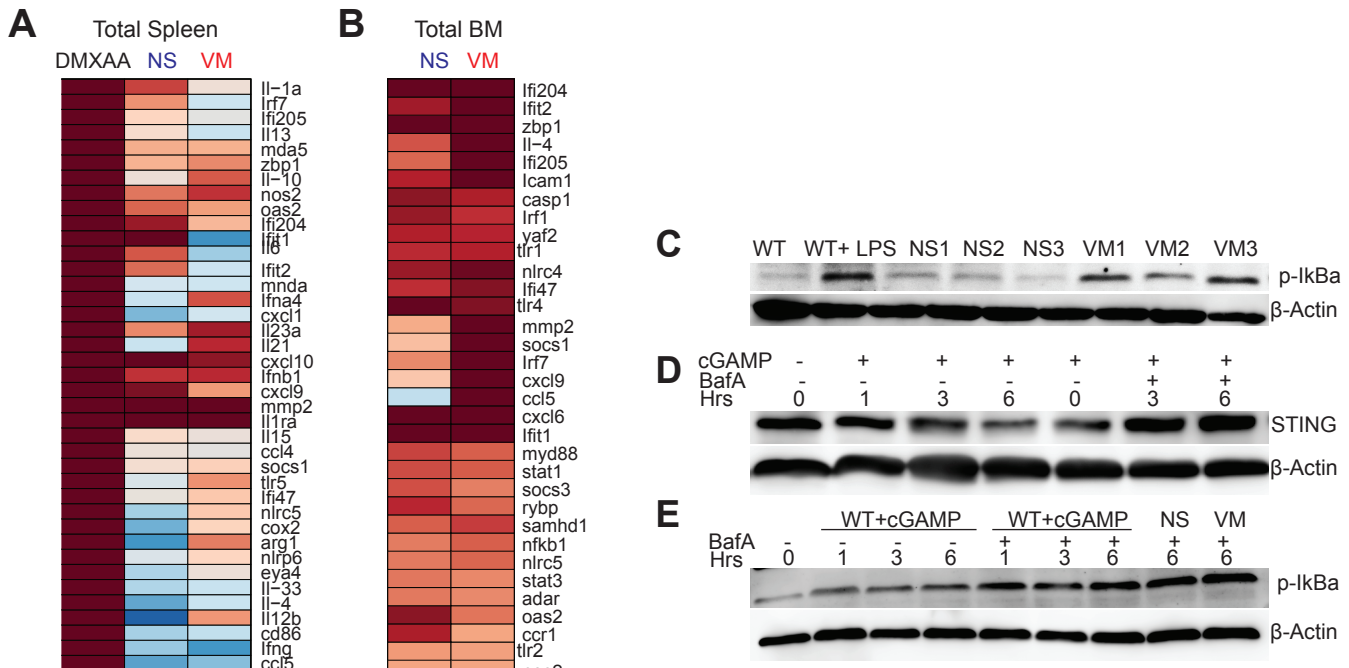

Fig. S2. SAVI mutant mice express interferon and inflammatory gene signature

RNA from total spleen (**A**) and total bone marrow (**B**) was isolated from 4-6 weeks old mice and mRNA profiling of ISGs was performed using nanostring technology. The data obtained was normalized and fold change was calculated over reads from WT mice. DMXAA was injected IP at 10mg/ml, 50ul/mouse for 8 hours and RNA from total spleen was used.
(**C**) BMDM lysates were prepared from 5-6 weeks old WT, N153S or V154M HET mice and probed for pIkBa and actin as loading control. WT cells treated with 100ng LPS for 30 min were used as positive control. (**D**) WT BMDMs transfected with 2ug/ml cGAMP were either untreated or treated with 5um Bafilomycin A for the indicated time points and total cell lysates were probed for STING and actin as loading control. (**E**) pIkBa levels were measured in total cell lysates in WT BMDMs transfected with 2ug/ml cGAMP as well as N153S and V154M mutant BMDMs treated with 5um Bafilomycin A for indicated time points.

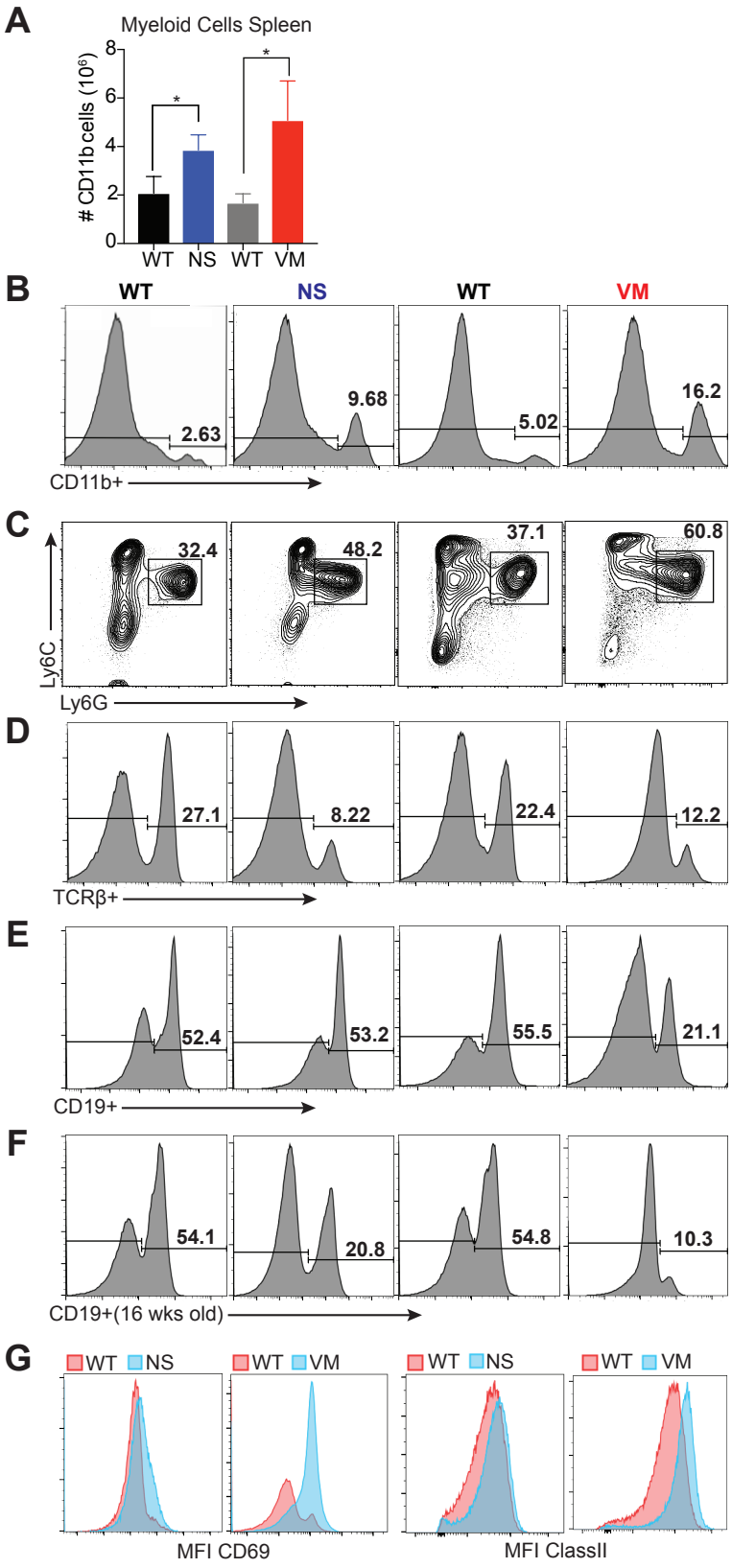

Fig. S3. V154M mutant presents severe immune cell alterations as compared to N153S SAVI mutant mice

Quantification of CD11b+ myeloid cell numbers in the spleen is shown (**A**). Representative flow plots for litter mate WT and respective SAVI mutants that were 6 weeks old, myeloid cells were identified as CD11b+ (**Panel B**), CD11b+ Ly6Ghi were used as markers to identify percent neutrophils (**Panel C**) percentages of splenic T cells were calculated by TCRb+ staining (**Panel D**) CD19+ were quantified as percent in SAVI mutants and their respective WT littermate controls (**Panel E**). Spleens from 16-20 weeks old mice were analyzed for CD19+ cells and quantified as percent (**Panel F**). The activation status of T cells was measured using mean fluorescence intensity of CD69 and MHC Class II on CD19+ cells was used as activation marker for B cells (**Panel G**).

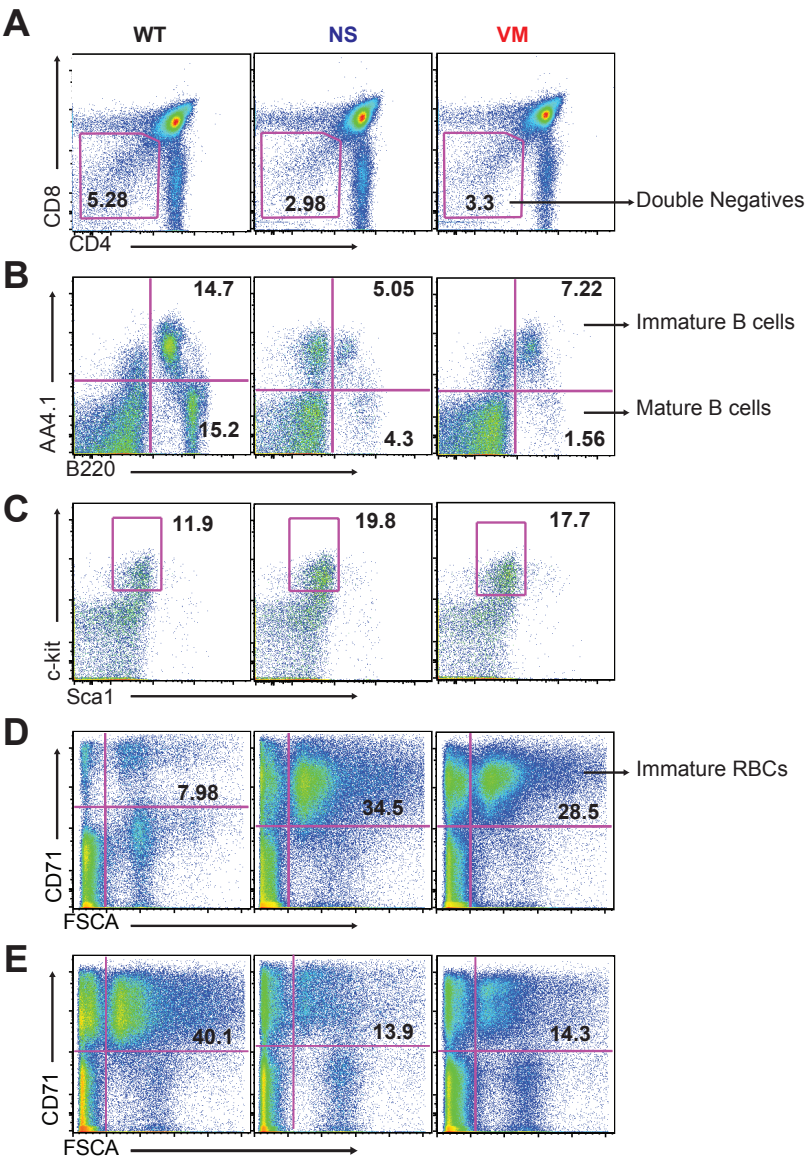

Fig. S4. SAVI mutations cause abnormal lymphocyte development

Representative flow plots for litter mate WT and respective SAVI mutants for percentages of CD4-CD8- double negatives in thymus (**A**). Bone marrow of 16-20-week-old mice were analyzed for immature or mature B cells (**B**). Representative flow plots for myeloid progenitors as characterized by lin-sca1-ckit+ (**C**). Spleen (**D**) and bone marrow were analyzed for percentages of immature RBCs as characterized by Ter119+CD71+ (E).

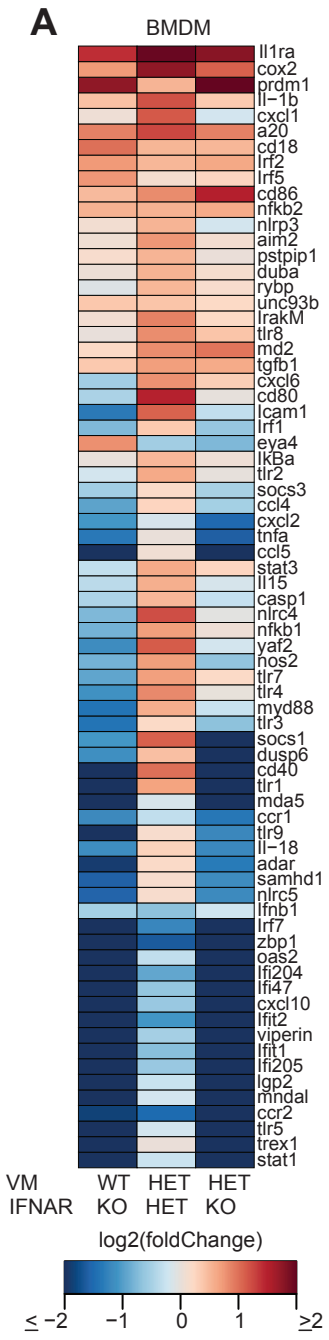

Fig. S5. IRF3, IFNAR and MLKL deficiency fail to rescue V154M SAVI phenotype

(**A**) RNA from bone marrow derived macrophages was isolated and mRNA profiling of ISGs was performed using Nanostring technology. The data obtained was normalized and fold change was calculated over reads from WT mice.

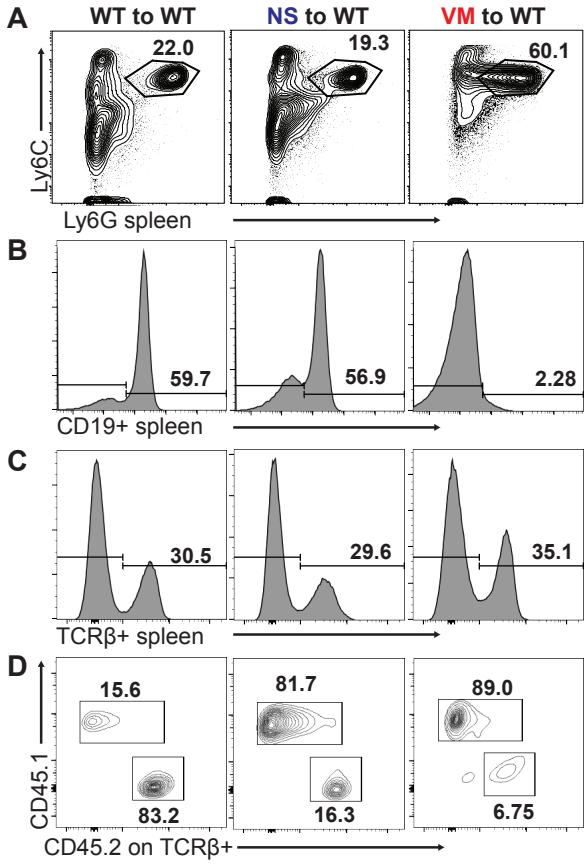

Fig. S6. Bone Marrow chimeras reveal distinct disease outcomes between the N153S and V154M mutant mice

Percentage of CD11b+ Ly6Ghi neutrophils in spleen for WT to WT, NS into WT and VM into WT chimeric strains (**A**). Flow plots for CD19 + B cells (**B**) and TCRb+ T cell percentages from spleen are shown (**C**). Within the splenic TCRb+ gate, CD45.2+, CD45.1+ cells were analyzed to obtain percentages of donor or recipient derived T cells respectively (**D**). The analysis was performed on reconstituted mice, 8-10 weeks after the bone marrow transplants. The chimera experiment was repeated twice with n=8-10 mice per genotype.

Supplementary Tables:

Table S1: Histology evaluation (H&E) of tissues in aged SAVI mice

	Liver n=5 (16 weeks)	Kidney n=5 (16 weeks)	Heart n=5 (16 weeks)	Lung n= 5 mice (8-24 weeks) Inflammation	Lung n= 5 mice (10-24 weeks) Fibrosis
WT	0	0	0	0	0
N153S	2	0	0	6	0
V154M	2	0	0	11	5

Average score of inflammation in total of 5 mice, scoring scale as described in (1, 2)

Table S2: Summary of lung disease in SAVI patients with various STING mutations

References	**STING Mutation**	**No. of patients**	**Lung disease**	**Direct comparison of V155M and N154S STING mutants**
Liu et al. (3)	V147L	1	No Interstitial lung disease/No fibrosis	Enhanced IFNβ promoter activity in V155M as compared to N154S
	N154S	4	2/4 Interstitial lung disease and fibrosis	
	V155M	1	Interstitial lung disease and fibrosis	
Chia et al. (4)	N154S	1	Interstitial lung disease/ND	N/A
Clarke et al. (5)	V155M	1	Interstitial lung disease/ND	N/A
Omoyinmi et al. (6)	V155M	1	Interstitial lung disease and fibrosis	N/A
Yu et al. (7)	V155M	1	Interstitial lung disease and pulmonary hypertension	N/A
Jeremiah et al. (8)	V155M	4	3/4 Interstitial lung disease and fibrosis	N/A
Picard et al. (9)	V155M	3	Interstitial lung disease and fibrosis	N/A
Munoz et al. (10)	V147M	1	Interstitial lung disease/ND	N/A
Melki et al. (11)	R281Q	1	Interstitial lung disease and fibrosis	N/A
	R284G	1	Normal Lung Function	N/A
	C206Y	1	Normal Lung Function	N/A
Saldhanha et al. (12)	R284S	1	Pulmonary hypertension	N/A
Konno et al. (13)	R284S	1	ND	N/A
König et al. (14)	G166E	5	No Interstitial lung disease	Increased production of IFNβ in N154S as compared to G166E

Supplementary References:

1. Curtis JL, Byrd PK, Warnock ML, & Kaltreider HB (1991) Requirement of CD4-positive T cells for cellular recruitment to the lungs of mice in response to a particulate intratracheal antigen. *J Clin Invest* 88(4):1244-1254.
2. Ashcroft T, Simpson JM, & Timbrell V (1988) Simple method of estimating severity of pulmonary fibrosis on a numerical scale. *Journal of clinical pathology* 41(4):467-470.
3. Liu Y*, et al.* (2014) Activated STING in a vascular and pulmonary syndrome. *N Engl J Med* 371(6):507-518.
4. Chia J*, et al.* (2016) Failure to thrive, interstitial lung disease, and progressive digital necrosis with onset in infancy. *J Am Acad Dermatol* 74(1):186-189.
5. Clarke SL*, et al.* (2016) Interstitial Lung Disease Caused by STING-associated Vasculopathy with Onset in Infancy. *American journal of respiratory and critical care medicine* 194(5):639-642.
6. Omoyinmi E*, et al.* (2015) Stimulator of interferon genes-associated vasculitis of infancy. *Arthritis & rheumatology* 67(3):808.
7. Yu ZX*, et al.* (2018) [Stimulator of interferon genes-associated vasculopathy with onset in infancy: first case report in China]. *Zhonghua er ke za zhi = Chinese journal of pediatrics* 56(3):179-185.
8. Jeremiah N*, et al.* (2014) Inherited STING-activating mutation underlies a familial inflammatory syndrome with lupus-like manifestations. *J Clin Invest* 124(12):5516-5520.
9. Picard C*, et al.* (2016) Severe Pulmonary Fibrosis as the First Manifestation of Interferonopathy (TMEM173 Mutation). *Chest* 150(3):e65-71.
10. Munoz J*, et al.* (2015) Stimulator of Interferon Genes-Associated Vasculopathy With Onset in Infancy: A Mimic of Childhood Granulomatosis With Polyangiitis. *JAMA Dermatol* 151(8):872-877.
11. Melki I*, et al.* (2017) Disease-associated mutations identify a novel region in human STING necessary for the control of type I interferon signaling. *J Allergy Clin Immunol* 140(2):543-552 e545.
12. Saldanha RG*, et al.* (2018) A Mutation Outside the Dimerization Domain Causing Atypical STING-Associated Vasculopathy With Onset in Infancy. *Frontiers in immunology* 9:1535.
13. Konno H*, et al.* (2018) Pro-inflammation Associated with a Gain-of-Function Mutation (R284S) in the Innate Immune Sensor STING. *Cell reports* 23(4):1112-1123.
14. Konig N*, et al.* (2017) Familial chilblain lupus due to a gain-of-function mutation in STING. *Annals of the rheumatic diseases* 76(2):468-472.